FEBS Letters 539 (2003) 138–142 FEBS 27087

Solution structure of CnErg1 (Ergtoxin), a HERG specific scorpion toxin

Allan M. Torres[a,*], Paramjit Bansal[b], Paul F. Alewood[b], Jane A. Bursill[c], Philip W. Kuchel[a], Jamie I. Vandenberg[c]

[a] *School of Molecular and Microbial Biosciences, University of Sydney, NSW 2006, Australia*
[b] *Institute for Molecular Bioscience, University of Queensland, St. Lucia, Qld 4072, Australia*
[c] *Victor Chang Cardiac Research Institute and Department of Medicine, University of New South Wales, 384 Victoria Street, Darlinghurst, NSW 2010, Australia*

Received 13 December 2002; revised 18 February 2003; accepted 18 February 2003

First published online 5 March 2003

Edited by Stuart Ferguson

Abstract The three-dimensional structure of chemically synthesized CnErg1 (Ergtoxin), which specifically blocks HERG (human *ether-a-go-go*-related gene) K^+ channels, was determined by nuclear magnetic resonance spectroscopy. CnErg1 consists of a triple-stranded β-sheet and an α-helix, as is typical of K^+ channel scorpion toxins. The peptide structure differs from the canonical structures in that the first β-strand is shorter and is nearer to the second β-strand rather than to the third β-strand on the C-terminus. There is also a large hydrophobic patch on the surface of the toxin, surrounding a central lysine residue, Lys13. We postulate that this hydrophobic patch is likely to form part of the binding surface of the toxin.

Key words: Ergtoxin; Human *ether-a-go-go*-related gene; K^+ ion channel; Chemical synthesis; NMR structure

1. Introduction

Recently, a new class of peptides from scorpion venom that specifically affect K^+ channels of the *ether-a-go-go*-related family of genes has been discovered and characterized [1–3]. This novel γ-Ktx family [4] includes potent peptides such as CnErg1 (previously known as ErgTx [1]), BeKm-1 [5] and CsEKerg1 [6], whose sequences range from 36 to 47 amino acid residues. Structural studies on BeKm-1 toxin show that it contains an α-helix and a triple-stranded β-sheet, typical of K^+ channel scorpion toxins [7]. Interestingly, the most important residues for toxin activity, Lys18 and Tyr11, are located on the α-helix of BeKm-1, rather than the solvent-exposed surface of the β-sheet which is more typical of scorpion K^+ channel toxins [8,9]. Moreover, the separation of these two residues is ~12 Å, i.e. significantly greater than the 6.6 ± 1.0 Å typical of the functional dyad of scorpion toxins that block K^+ channels [8]. There is, however, an additional aromatic residue on the α-helix of BeKm-1, Phe14, that lies approximately 6 Å from Lys18 and so Phe14/Lys18 may serve as the functional dyad for BeKm-1 [7]. Nevertheless, the binding surface of BeKm-1 appears to be quite distinct from that of other scorpion K^+ channel toxins.

The human *ether-a-go-go*-related gene (HERG) K^+ channel is an important contributor to normal cardiac repolarization [10]. Furthermore, loss-of-function mutations in the HERG K^+ channel are the cause of long QT syndrome type-2, which is associated with a markedly increased risk of ventricular arrhythmias and sudden death [11]. One of the distinctive features of the HERG K^+ channel is a long extracellular loop linking the outer ends of the fifth transmembrane domain and the pore helix (S5-P loop) [12]. Mutations in this loop affect the rapid voltage dependent inactivation of the HERG K^+ channel that is critical for its normal function [13].

CnErg1, like BeKm-1, binds to the S5-P loop of the HERG K^+ channel [7,12]. Although CnErg1 and BeKm-1 are functionally both members of the γ-Ktx family they share little sequence homology and contain four and three disulfide bonds, respectively (Fig. 1A). Knowledge of the structure of CnErg1 should therefore provide complementary structural information and together with the BeKm-1 structure [7] should help in mapping the HERG K^+ channel outer vestibule, which is critically important for the unique function of this channel.

We report here the three-dimensional fold of chemically synthesized CnErg1 through the use of nuclear magnetic resonance (NMR) spectroscopy. CnErg1 adopts an α-helix triple-stranded β-sheet conformation typical of K^+ channel scorpion toxins. Lys25 and Tyr17 in CnErg1 occur on the α-helix in a similar orientation to that of Lys18 and Tyr11 in BeKm-1, i.e. the residues most critical for activity of BeKm-1. However, CnErg1 also contains a hydrophobic patch surrounding a lysine residue, Lys13, located near the β-hairpin loop between the second and third strands of the β-sheet which we postulate may represent the binding site of CnErg1.

2. Materials and methods

2.1. Synthesis of CnErg1 and preparation of NMR sample

CnErg1 was synthesized manually on a 0.50 mmol scale using HBTU (2-(1-H-benzotriazol-1-yl-)1,1,3,3 tetramethyluronium hexafluorophosphate) activation of Boc-amino acids with in situ neutralization chemistry as previously described [14]. Following HF cleavage, the reduced peptides were isolated and purified using reverse-phase high-performance liquid chromatography (RP-HPLC) using a C4 column. Disulfide bond formation was carried out in 100 mM ammo-

*Corresponding author. Fax. (61)-2-9351 4726.
E-mail address: a.torres@mmb.usyd.edu.au (A.M. Torres).

Abbreviations: HERG, human *ether-a-go-go*-related gene; NOESY, nuclear Overhauser enhancement spectroscopy; rmsd, root-mean-square deviation; TOCSY, total correlation spectroscopy

0014-5793/03/$22.00
doi:10.1016/S0014-5793(03)00216-3

nium acetate (pH 7.5) and the final purified products were isolated by preparative RP-HPLC as follows: fractions were collected, based on monitoring the column effluent at 230 nm. Those fractions shown by electrospray mass spectrometry analysis to contain solely the target peptide were combined and lyophilized.

The NMR sample was prepared by dissolving 2.9 mg of the lyophilized peptide in 0.350 ml of 90% H_2O/10% D_2O, resulting in a final protein concentration of 1.7 mM and pH 3.2.

2.2. NMR spectroscopy

All NMR experiments were performed on a Bruker (Karlsruhe, Germany) AVANCE-600 DRX spectrometer using a 5 mm ^{1}H inverse probe operating at temperatures of 20, 25, and 30°C. Two-dimensional NMR spectra were acquired in phase-sensitive mode using time-proportional phase detection [15]. The homonuclear two-dimensional spectra recorded were total correlation spectroscopy (TOCSY) [16], with spin-lock periods of 60 ms, and nuclear Overhauser enhancement spectroscopy (NOESY) [17] with mixing times of 200 ms. Solvent-signal suppression was achieved either by presaturation or by using the WATERGATE [18] pulse sequence. H–D exchange experiments were carried out by reconstituting the freeze-dried sample with D_2O, acquiring series of one-dimensional spectra for 30 min, and then acquiring two 1 h TOCSY spectra. All spectra were processed using XWIN-NMR software (Bruker) and were analyzed using the program XEASY [19].

2.3. Structural calculations

The structure was obtained by using restraints consisting of 535 non-redundant NOE-derived distances, 32 hydrogen bonds, 11 ϕ dihedral angles and 4 disulfide bonds (see Table 1). The NOESY spectrum recorded at 25°C with a mixing time of 200 ms provided the NOE and dihedral angle constraints. The program INFIT [20] was implemented to yield $^3J_{NH\alpha}$ coupling constants from two-dimensional NOESY spectra, which then provided ϕ dihedral angle constraints which were restrained as follows: $-120 \pm 30°$ for $^3J_{NH\alpha} = 8$–9 Hz and $-60 \pm 40°$ for $^3J_{NH\alpha} = 5$–6 Hz. Hydrogen-bonding pairs were deduced from H–D exchange experiments, and the preliminary calculated structures. Hydrogen-bonding constraints were only introduced in the final stages of the structure calculations and were assigned upper distance-limits of 2.2 Å for NH_i to O_j and 3.2 Å for N_i to O_j. The disulfide bond configuration was determined from the characteristic NOE interactions between the α and β protons of two-paired cysteine residues. A summary of the NMR data for CnErg1 is presented in Fig. 2.

The NOAH protocol [21,22] in the torsion-angle dynamics program DYANA [23] was used in calculating preliminary structures and in assigning about 50% of non-intra-residue NOESY cross-peaks. The standard simulated annealing procedure in DYANA was afterwards implemented to improve the quality of structures by performing an iterative cycle of calculations, structure analysis, manual assignment, and constraint revision. Final DYANA calculation yielded 4000 structures, 80 of which (with the lowest NOE violations) were chosen for refinement by using the standard simulated annealing script in CNS [24]. In this refinement process, the high-temperature dynamics and cooling cycle were performed in Cartesian space. The 20 structures with the lowest overall energy were considered as representative of CnErg1. Secondary structures in CnErg1 were determined using MOLMOL [25].

The coordinates for the ensemble of 20 structures, including the structural restraints, have been deposited in the RSCB Protein Data Bank with accession code 1NE5. The chemical shift assignments were deposited in the BioMagRes Bank with accession number 5652.

2.4. Electrophysiology

CHO cells stably transfected with HERG K^+ channels [26] were voltage clamped in whole cell mode using an Axopatch 200B headstage amplifier (Axon instruments, CA, USA), as previously described [27]. Currents were digitized on line using a digidata 1200 A/D converter (Axon instruments, CA, USA) operated using pClamp8 software. The internal solution contained (in mM): 120 K gluconate, 20 KCl, 1.5 MgATP, 5 EGTA, 10 HEPES (pH 7.3 with KOH). The bath solution contained 130 NaCl, 4.8 KCl, 1.2 $MgCl_2$, 1.2 NaH_2PO_4, 1 $CaCl_2$, 10 glucose, 10 HEPES (titrated to pH 7.3 with NaOH) at room temperature. CnErg1 was dissolved directly in bath solution at doses ranging from 3 nM to 1 μM and applied using a picospritzer (Intracell, Cambridge, UK).

3. Results and discussion

3.1. Verification of synthetic peptide

The amino acid sequence of the peptide synthesized in this study is shown in Fig. 1A. Also shown are the disulfide bond pairings (5–23, 11–34, 20–39 and 24–41) as reported by Scaloni et al. [2]. With the absence of the native material for comparison, the synthetic CnErg1 peptide was first tested for activity to confirm that it was identical to that of the native toxin. HERG K^+ channel activity was suppressed ~50% by 10 nM toxin (see Fig. 1B). The IC_{50} for inhibition of HERG channels was 8.5 ± 1.0 nM ($n = 3$, see Fig. 1C) with a maximum inhibition of $94 \pm 1\%$ both of which are very similar to that reported in the literature [3,12]. We also found that the observed NOEs in the NMR experiments were consistent with the cysteine pairing pattern reported by Scaloni et al. [2]. Thus, this synthetic peptide was concluded to be equivalent to the native material.

3.2. Overall fold and secondary structures

The ^{1}H NMR spectra obtained from the CnErg1 were of high quality, making the analysis straightforward and yielding a high-resolution structure. This is clearly exemplified by the ensemble of the 20 NMR structures shown in Fig. 3A. The overall backbone root-mean-square deviation (rmsd) with respect to the mean structure for residues 5–42 was 0.25 Å while the corresponding heavy atom rmsd for these residues was 0.71 Å (Table 1).

The CnErg1 structure starts with a flexible N-terminal up to residue 4 and is then followed by a turn-like structure, likely to be a 3_{10} helix, at residues 5–7. The first β-strand of the triple-stranded antiparallel β-sheet is short, formed by residues 14–15. The remaining two antiparallel β-strands are defined by residues 32–35 and 39–41; with an intervening β-hairpin loop at residues 35–37. An α-helix, formed by residues 18–27, follows the first β-strand and traverses the three β-strands diagonally (see Fig. 3B). The overall fold of CnErg1, with a distinct α-helix and triple-stranded β-sheet, is similar to other scorpion toxins that affect K^+ and Na^+ channels [4]. The CnErg1 structure, however, is unusual among scorpion K^+ channel toxins in that a turn or a short helix is situated at the N-terminal end of the peptide instead of the more usual first strand of the β-sheet. Moreover, the first β-strand in CnErg1 interacts (by hydrogen bond) with the second

Table 1
Structural statistics for the ensemble of 20 CnErg1 structures

Quantity	Value
Distance restraints	
Intraresidue ($i-j=0$)	207
Sequential ($\|i-j\|=1$)	134
Medium range ($\|i-j\| \le 5$)	76
Long range ($\|i-j\| > 5$)	118
Hydrogen bonds	32
Total	567
Dihedral angle restraints	
ϕ	11
Atomic rmsd with the mean structure (Å)	
Backbone atoms (1–42)	0.57 ± 0.30
Heavy atoms (1–42)	1.15 ± 0.37
Backbone atoms (5–42)	0.25 ± 0.04
Heavy atoms (5–42)	0.71 ± 0.09

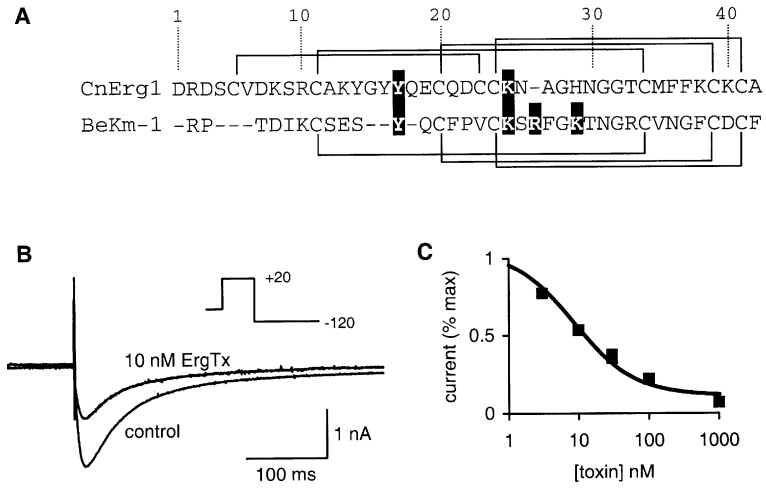

Fig. 1. Functional assessment of chemically synthesized CnErg1. A: Sequence alignment of CnErg1 (Ergtoxin) and BeKm-1 showing the predicted disulfide bridges. The highlighted residues indicate those most important for BeKm-1 activity (Tyr11, Lys18, Arg20, Lys23) [7]. Tyr11 and Lys18 are conserved in CnErg1 (Tyr17 and Lys25). Alignment was performed using Clustal W [33]. The numbering above the sequences corresponds to CnErg1. B: Representative current traces from a CHO cell transfected with HERG K^+ channels. During a depolarization step from −80 to +20 mV channels open and then inactivate. During the subsequent repolarization step to −120 mV the currents show the characteristic 'hook' as channels rapidly recover from the inactive state into the open state before closing slowly. In this example, addition of 10 nM CnErg1 caused 52% inhibition of the current. C: Dose response curve for CnErg1 blockade of HERG K^+ channels. The continuous curve shows the best fit for the equation: % max current = $1-A([\text{toxin}]/([\text{toxin}]+K_d))$, where A is the maximum inhibition (94 ± 1%, $n=3$) and K_d is the affinity of toxin for the HERG K^+ channel (8.5 ± 1.0 nM, $n=3$).

β-strand and not the third β-strand, as found in many common scorpion toxins [9].

A DALI algorithm [28] search of similar structures in the protein database revealed that the structural fold of CnErg1 has significant similarity to that of OSK1, a scorpion toxin from *Orhtochirus scrobiculosus* that blocks Ca^{2+}-activated K^+ channels [29]. Despite sequence identity of only 35%, about 80% of the residues in CnErg1 are found to be structurally equivalent to that of OSK1. However, since important residues Lys27, Asn30, Gly31, His34, and Thr36 in OSK1 are different from the corresponding residues in CnErg1, it can be surmised that the binding sites for these two K^+ channel molecules are different.

3.3. Structural implications

It has been proposed that that the ability of unrelated toxins to recognized voltage-activated K^+ channels is due to the presence of a dyad comprising of a lysine residue and an aromatic residue separated by 6.6 ± 1.0 Å [8]. Many of the short scorpion K^+ channel toxins have these two important residues residing on the solvent-exposed surface of the flat β-sheet face [8]. BeKm-1, which shares a common structural scaffold with other short scorpion toxins, is different in that its binding site for the HERG K^+ channel is situated on the helix [7]. Furthermore, while the most critical lysine residue, Lys18, in BeKm-1 is located ~6 Å from an aromatic residue, Phe14, the aromatic residue most critical for function of the toxin, Tyr11, is located near the N-terminus of the helix and is situated ~12 Å from Lys18. The corresponding residues in CnErg1, Lys25, Gln21 and Tyr17, are also located on the helical part of the molecule. Clearly, Gln21 cannot fulfil the role of a functional dyad. Conversely, Lys38 which lies along the β-sheet plane of the molecule, pointing towards the solvent (see Fig. 3C), is separated from Phe36 on the β-hairpin loop by ~7 Å and easily satisfies the criterion of the functional dyad. Furthermore, Lys13 lies within 7 Å of Tyr14, Phe36 and Phe37. Thus there are at least two potential functional dyads present in CnErg1. Clarification of the role of these potential dyads and the α-helix as putative binding sites (as is the case for BeKm-1) will require future mutagenesis studies.

The binding of K^+ channel specific scorpion toxins to their receptors on the outer vestibule of the channel pore involves a

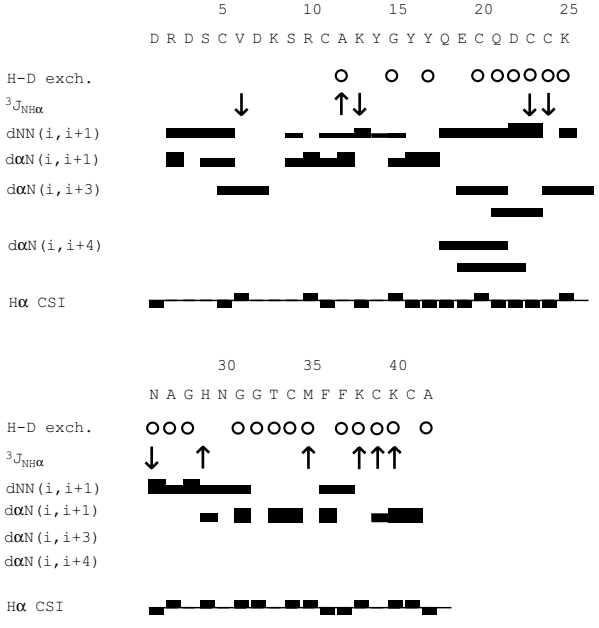

Fig. 2. Summary of NMR data for Cnerg1. Slowly exchanging backbone amides at 25°C are indicated by circles, $^3J_{NH\alpha}=8$–9 Hz by upward pointing arrows, and $^3J_{NH\alpha}=5$–6 Hz by downward pointing arrows. Each NOE connectivity is represented by a shaded horizontal bar whose thickness is proportional to the observed NOE intensity; Hα chemical shift indices (CSI) [34] are indicated by vertical bars.

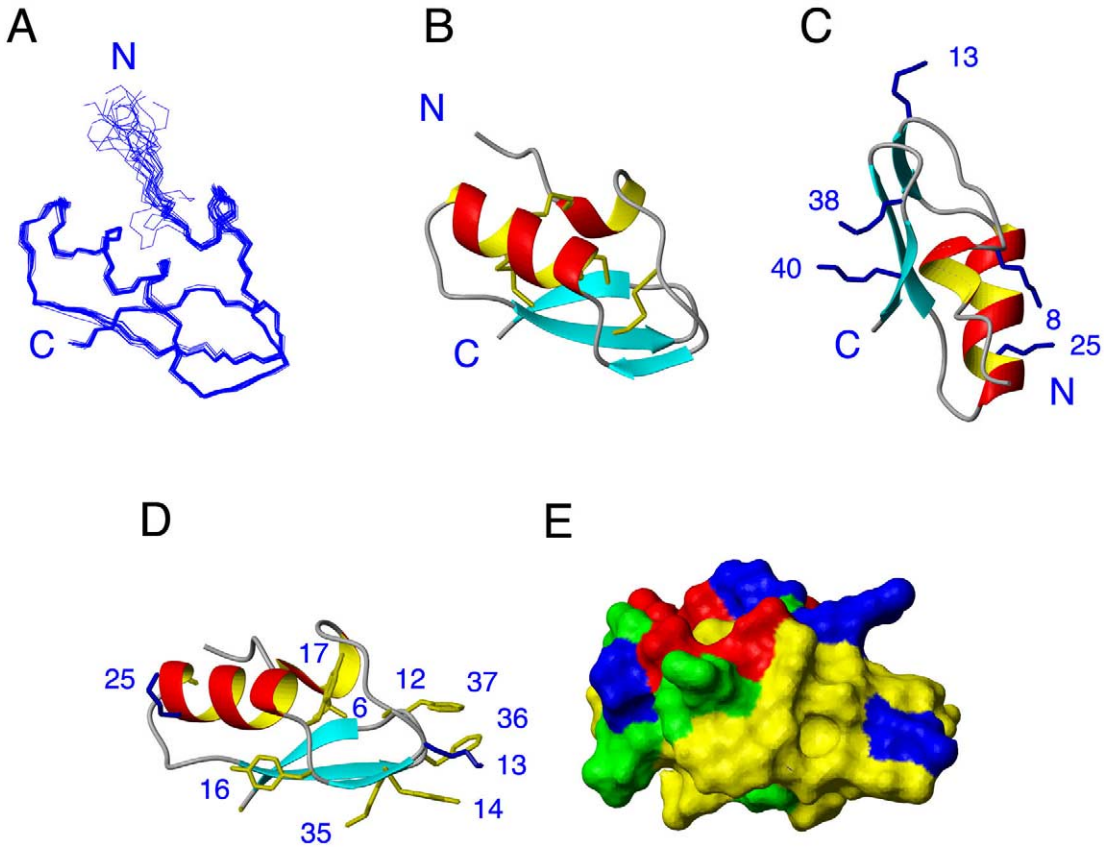

Fig. 3. The CnErg1 structure. A: Ensemble of the best 20 CnErg1 structures aligned by superimposing backbone atoms of residues 5–42. B: Ribbon diagram showing secondary structures and disulfide connectivities. C: Different view of the structure emphasizing the side-chains of lysine residues. D: Ribbon diagram showing locations of important residues. Side-chain heavy atoms of Lys13 and Lys25 are shown in blue while those of non-polar and Tyr residues are shown in yellow. E: Molecular surface showing hydrophilicity/hydrophobicity. The types of residues are distinguished by their color: non-polar and Tyr residues – yellow; polar uncharged residues – green; positively charged – blue; and negatively charged – red. The figures were generated using MOLMOL [25].

combination of hydrophobic, hydrogen bonding, and electrostatic interactions [30–32]. The binding of Ergtoxin to HERG channels, however, is not influenced by the extracellular [K^+] and does not involve strong electrostatic interactions [12]. It is therefore likely that hydrophobic interactions will play a more important role in Ergtoxin binding to HERG than is the case for other scorpion toxins binding to their respective ion-channel receptors. A notable feature of the CnErg1 structure is the presence of a large hydrophobic patch centered around an aromatic cluster defined by Tyr 14, Phe 36 and Phe 37 (see Fig. 3D,E). Furthermore, in the middle of this hydrophobic patch lies Lys13. It has been suggested that CnErg1 binds to the hydrophobic surface of an amphipathic helix in the outer vestibule of the HERG K^+ channel [12]. It has been shown that mutations of hydrophobic residues on a putative amphipathic helix in the extracellular linker between the fifth transmembrane domain and the pore helix (S5-P linker) significantly decrease the affinity of CnErg1 for the HERG K^+ channel [12]. Therefore, it is possible that hydrophobic interactions may make a significant contribution to the interaction of CnErg1 with the HERG K^+ channel.

Another interesting structural feature of CnErg1 is the presence of numerous acidic residues (Asp1, Asp3, Asp7, Asp22, and Glu19) located on or near the helical side, opposite the triple-stranded β-sheets. While few positively charged residues are also present in this face of the molecule, it is nevertheless possible that these negatively charged residues are important in binding positively charged residues. Alternatively, they may be involved in reorientating the CnErg1 as it docks to the HERG K^+ channel outer vestibule. The outer vestibule of the HERG K^+ channel contains numerous positively charged residues including Arg582, Lys595, Lys608, Lys610 and Lys638 [12]. Cysteine mutants of Arg582, Lys608 and Lys610 did not affect the affinity of CnErg1. Cysteine mutants of Lys595 and Lys638, however, were non-functional so it is possible that these residues could be involved in toxin binding. Confirmation of whether the charged residues in CnErg1 contribute to docking of the toxin to the channel will be tested using mutant cycle analysis experiments.

In conclusion, we have shown that the CnErg1 has a structure broadly similar to other scorpion toxins that inhibit K^+ channels, containing a distinctive α-helix and triple-stranded β-sheet. However, there are some important differences most notable of which is a large, solvent-exposed, hydrophobic patch that could be important for docking CnErg1 to HERG. This structure provides a useful starting point for designing mutant cycle analysis experiments to help determine the structure of the outer vestibule of the HERG K^+ channel.

Acknowledgements: This work was supported by an Australian Research Council Grant to P.W.K. and an NH&MRC Project grant to J.I.V. J.I.V. is an NH&MRC R.D. Wright Fellow.

References

[1] Corona, M., Gurrola, G.B., Merino, E., Cassulini, R.R., Valdez-Cruz, N.A., Garcia, B., Ramirez-Dominguez, M.E., Coronas, F.I., Zamudio, F.Z., Wanke, E. and Possani, L.D. (2002) FEBS Lett. 532, 121–126.

[2] Scaloni, A., Bottiglieri, C., Ferrara, L., Corona, M., Gurrola, G.B., Batista, C., Wanke, E. and Possani, L.D. (2000) FEBS Lett. 479, 156–157.

[3] Gurrola, G.B., Rosati, B., Rocchetti, M., Pimienta, G., Zaza, A., Arcangeli, A., Olivotto, M., Possani, L.D. and Wanke, E. (1999) FASEB J. 13, 953–962.

[4] Tytgat, J., Chandy, K.G., Garcia, M.L., Gutman, G.A., Martin-Eauclaire, M.F., van der Walt, J.J. and Possani, L.D. (1999) Trends Pharmacol. Sci. 20, 444–447.

[5] Korolkova, Y.V., Kozlov, S.A., Lipkin, A.V., Pluzhnikov, K.A., Hadley, J.K., Filippov, A.K., Brown, D.A., Angelo, K., Strobaek, D., Jespersen, T., Olesen, S.P., Jensen, B.S. and Grishin, E.V. (2001) J. Biol. Chem. 276, 9868–9876.

[6] Nastainczyk, W., Meves, H. and Watt, D.D. (2002) Toxicon 40, 1053–1058.

[7] Korolkova, Y.V., Bocharov, E.V., Angelo, K., Maslennikov, I.V., Grinenko, O.V., Lipkin, A.V., Nosyreva, E.D., Pluzhnikov, K.A., Olesen, S.P., Arseniev, A.S. and Grishin, E.V. (2002) J. Biol. Chem. 277, 43104–43109.

[8] Dauplais, M., Lecoq, A., Song, J.X., Cotton, J., Jamin, N., Gilquin, B., Roumestand, C., Vita, C., Demedeiros, C.L.C., Rowan, E.G., Harvey, A.L. and Menez, A. (1997) J. Biol. Chem. 272, 4302–4309.

[9] Tenenholz, T.C., Klenk, K.C., Matteson, D.R., Blaustein, M.P. and Weber, D.J. (2000) Rev. Physiol. Biochem. P. 140, 135–185.

[10] Sanguinetti, M.C., Jiang, C., Curran, M.E. and Keating, M.T. (1995) Cell 81, 299–307.

[11] Vandenberg, J., Walker, B. and Campbell, T. (2001) Trends Pharmacol. Sci. 22, 240–246.

[12] Pardo-Lopez, L., Zhang, M., Liu, J., Jiang, M., Possani, L.D. and Tseng, G.N. (2002) J. Biol. Chem. 277, 16403–16411.

[13] Liu, J., Zhang, M., Jiang, M. and Tseng, G.N. (2002) J. Gen. Physiol. 120, 723–737.

[14] Schnolzer, M., Alewood, P., Jones, A., Alewood, D. and Kent, S.B.H. (1992) Int. J. Peptide Protein Res. 40, 180–193.

[15] Marion, D. and Wüthrich, K. (1983) Biochem. Biophys. Res. Commun. 113, 967–974.

[16] Bax, A. and Davis, D.G. (1985) J. Magn. Reson. 65, 355–360.

[17] Kumar, A., Ernst, R.R. and Wüthrich, K. (1980) Biochem. Biophys. Res. Commun. 95, 1–6.

[18] Piotto, M., Saudek, V. and Sklenar, V. (1992) J. Biomol. NMR 2, 661–665.

[19] Bartels, C., Xia, T.H., Billeter, M., Guntert, P. and Wüthrich, K. (1995) J. Biomol. NMR 6, 1–10.

[20] Szyperski, T., Guntert, P., Otting, G. and Wüthrich, K. (1992) J. Magn. Reson. 99, 552–560.

[21] Mumenthaler, C., Guntert, P., Braun, W. and Wüthrich, K. (1997) J. Biomol. NMR 10, 351–362.

[22] Mumenthaler, C. and Braun, W. (1995) J. Mol. Biol. 254, 465–480.

[23] Guntert, P., Mumenthaler, C. and Wüthrich, K. (1997) J. Mol. Biol. 273, 283–298.

[24] Brunger, A.T., Adams, P.D., Clore, G.M., DeLano, W.L., Gros, P., Grosse-Kunstleve, R.W., Jiang, J.S., Kuszewski, J., Nilges, M., Pannu, N.S., Read, R.J., Rice, L.M., Simonson, T. and Warren, G.L. (1998) Acta Crystallogr. D 54, 905–921.

[25] Koradi, R., Billeter, M. and Wüthrich, K. (1996) J. Mol. Graph. 14, 51–5.

[26] Walker, B.D., Valenzuela, S.M., Singleton, C.B., Tie, H., Bursill, J.A., Wyse, K.R., Qiu, M.R., Breit, S.N. and Campbell, T.J. (1999) Br. J. Pharmacol. 127, 243–251.

[27] Lu, Y., Mahaut-Smith, M.P., Varghese, A., Huang, C.L., Kemp, P.R. and Vandenberg, J.I. (2001) J. Physiol. 537, 843–851.

[28] Holm, L. and Sander, C. (1993) J. Mol. Biol. 233, 123–138.

[29] Jaravine, V.A., Nolde, D.E., Reibarkh, M.J., Korolkova, Y.V., Kozlov, S.A., Pluzhnikov, K.A., Grishin, E.V. and Arseniev, A.S. (1997) Biochemistry 36, 1223–1232.

[30] Eriksson, M.A.L. and Roux, B. (2002) Biophys. J. 83, 2595–2609.

[31] MacKinnon, R. and Miller, C. (1988) J. Gen. Physiol. 91, 335–349.

[32] Ranganathan, R., Lewis, J.H. and MacKinnon, R. (1996) Neuron 16, 131–139.

[33] Thompson, J.D., Higgins, D.G. and Gibson, T.J. (1994) Nucleic Acids Res. 22, 4673–4680.

[34] Wishart, D.S., Sykes, B.D. and Richards, F.M. (1992) Biochemistry 31, 1647–1651.